Inorg. Chem. **2009**, *48*, 2399−2406

Structural Versatility of the ε-$SmGa_x$ Phase: X-Ray, Electron Diffraction, and DFT Studies

Monique Tillard,* David Zitoun, and Claude Belin

Agrégats, Interfaces, Matériaux pour l'Énergie, Institut Charles Gerhardt, UMR 5253 CNRS UM2, CC015, Université de Montpellier 2, Sciences et Techniques du Languedoc, 2 Place Eugène Bataillon, 34095 Montpellier Cedex 5, France

Received July 23, 2008

Two new compounds, $SmGa_{2.67}$ (hexagonal, $P\bar{6}2c$, $Z = 15$, $a = 12.861(2)$, $c = 8.4402(8)$ Å) and $SmGa_{3.64}$ (orthorhombic, *Fmmm*, $Z = 24$, $a = 8.493(1)$, $b = 14.912(2)$, $c = 17.080(2)$ Å), have been synthesized and identified in the Sm−Ga system and their crystal structures solved and refined from single-crystal X-ray diffraction. These structures display consistent atomic disorder. Electronic structures have been calculated using first-principle DFT methods with ordered models. Atomic arrangements and bonding are analyzed on the basis of gallium partial anionic networks; they are compared with those of some analogous compounds in the other lanthanide−gallium systems.

Introduction

After the discovery of an unconventional superconductivity for $PuCoGa_5$, ternary systems R−M−Ga (R = rare earth, actinide, M = transition metal elements) have been extensively studied. For the system Sm−Co−Ga, 18 ternary phases were cited in the literature until our work gave evidence for three novel phases, $Sm_4Co_3Ga_{16}$, $SmCoGa_4$, and $SmCoGa_5$, having interesting structural and physical properties.[1] On the other hand, some attention was also paid to the Sm−Ga binary diagram established in 1979[2] that contains five line compounds: $SmGa_6$, $SmGa_2$, SmGa, Sm_5Ga_3, and Sm_3Ga. The structural type Ba_5Si_3 (instead of Cr_5B_3) was further assigned to Sm_5Ga_3,[3] and crystal structures of two additional Sm-rich compounds, Sm_3Ga_2[4] and Sm_9Ga_4,[5] were determined. $SmGa_2$, which melts congruently (1390 °C), is the most stable compound in the phase diagram, and it lies at the border of the ε-$SmGa_x$ phase domain ($2 < x < 4$). As suggested elsewhere[6] and confirmed below, the crystal structures established for compositions within the ε phase are reminiscent deviations from that of $SmGa_2$ (AlB_2-type). Interestingly, the pseudo-two-dimensional character of the ε-$SmGa_x$ associated with some covalent bonding brings a strong analogy with the MgB_2 compound, a superconductor at 40 K, in which strong B−B bonding has been suspected to play an important role in the superconductivity mechanism.[7,8]

Experimental Section

The ε-$SmGa_x$ and $CoGa_3$ phases were the only side products obtained during the arc-melting synthesis of $SmCoGa_5$ from the elements taken in stoichiometric proportions. After they were identified by X-ray powder diffraction, well-crystallized ε-$SmGa_x$ was obtained by a Ga-flux synthesis (3.5 atom % Sm) in a tantalum tube sealed under an argon atmosphere at both ends by arc welding. The Ta reactor, protected from oxidation at high temperatures inside an evacuated silica jacket, was heated up to 800 °C, kept for 15 h for homogenization, cooled at 30°/h to 580 °C for a 24 h annealing, and finally cooled at 10°/h to room temperature for crystallization. After centrifugation at 200 °C, a temperature that makes gallium fluent enough to allow the deposit of crystals, the Ta tube was cut at the bottom to recover the crystallized material. Several small

* To whom correspondence should be addressed. Phone: 33 4 67 14 48 97. Fax: 33 4 67 14 33 04. E-mail: mtillard@univ-montp2.fr.

(1) Jia, Y.; Belin, C.; Tillard, M.; Lacroix-Orio, L.; Zitoun, D.; Feng, G. *Inorg. Chem.* **2007**, *46*, 4177–86.
(2) Yatsenko, S. P.; Semyannikov, A. A.; Semenov, B. G.; Chuntonov, K. A. *J. Less-Common Metals* **1979**, *64*, 185–199.
(3) Feng, G. H.; Lacroix-Orio, L.; Tillard, M.; Belin, C. *Acta Crystallogr.* **2005**, *C61*, i71–i72.
(4) Yatsenko, S. P.; Gladyshevskii, R. E.; Sitschewitsch, O. M.; Belsky, V. K.; Semyannikov, A. A.; Grin, Y. N.; Yarmoluk, Y. P. *J. Less-Common Metals* **1986**, *115*, 17–22.
(5) Yatsenko, S. P.; Grin, Y.; Sitschewitsch, O. M.; Chuntonov, K. A.; Yarmoluk, Y. P. *J. Less-Common Metals* **1985**, *106*, 35–40.
(6) Grin, Y. N.; Fedorchuk, A. O. *Russ. Metall. (Engl. Transl.)* **1992**, *5*, 197–200.
(7) An, J. M.; Pickett, W. E. *Phys. Rev. Lett.* **2001**, *86*, 4366–4369.
(8) Nagamatsu, J.; Nakagawa, N.; Muranaka, T.; Zenitani, Y.; Akimitsu, J. *Nature* **2001**, *410*, 63.

10.1021/ic801379c CCC: $40.75
Published on Web 02/09/2009

Table 1. Crystallographic Details and Experimental Parameters for $SmGa_x$ Given Comparatively

cryst syst	orthorhombic	hexagonal	hexagonal
space group, number	*Fmmm*, 69	*P*312, 149	$P\bar{6}2c$, 190
unit cell dimensions (Å)	$a = 8.493(1)$	$a = 7.424(1)$	$a = 12.861(2)$
	$b = 14.912(2)$	$b = 7.424(1)$	$b = 12.861(2)$
	$c = 17.080(2)$	$c = 4.2176(6)$	$c = 8.4402(8)$
volume ($Å^3$)	2163.2(5)	201.29(5)	1209.06(3)
formula	$Sm_{0.98}Ga_{3.57}$ ("$SmGa_{3.64}$")	$Sm_{0.86}Ga_{2.41}$ ("$SmGa_{2.79}$")	$Sm_{1.06}Ga_{2.83}$ ("$SmGa_{2.67}$")
Z	24	3	15
fw	396.53	297.59	355.91
density	7.305	7.365	7.332
abs coeff (mm^{-1})	41.83	42.20	42.02
F(000)	4118	384	2297
cryst size (mm)	$0.10 \times 0.08 \times 0.07$	$0.14 \times 0.05 \times 0.03$	$0.14 \times 0.05 \times 0.03$
refinement method	full matrix least-squares on F^2	full matrix least-squares on F^2	full matrix least-squares on F^2
reflns collected	37159	3425	19637
θ range (deg)	3.01−31.99	3.17−32.14	3.0−32.3
independent reflns	1033 [$R_{int} = 0.038$]	465 [$R_{int} = 0.052$]	1466 [$R_{int} = 0.080$]
obsd reflns/refined params	860/52	318/31	985/61
extinction coeff ($\times 10^{-4}$)	1.1(1)	54(15)	9(6)
GOF on F^2	1.09	1.18	1.13
final indices R1[a] [$I > 2\sigma(I)$]	0.0394	0.0348	0.0540
wR2[a] [$I > 2\sigma(I)$]	0.1036	0.1143	0.1759
R1 (all data)	0.0502	0.0450	0.0884
wR2 (all data)	0.1064	0.1177	0.1944
largest diff. peak and hole ($e \cdot Å^{-3}$)	5.36/−3.17	1.99/−2.19	4.40/−3.71

[a] $R1 = \sum||F_o| - |F_c||/\sum|F_o|$, $wR2 = [\sum[w(F_o^2 - F_c^2)^2]/\sum[w(F_o^2)^2]]^{1/2}$.

shiny black crystals were selected under a microscope, mounted inside Lindemann capillaries, and tested on a CCD Xcalibur four-circle diffractometer (Oxford Diffraction) operating with monochromated Mo Kα radiation. Thereafter, it became evident that the product contained two varieties of crystals having almost the same appearance. Crystals checked for singularity display either orthorhombic or hexagonal symmetry.

Data collection on the CCD diffractometer was performed at room temperature over the angular 2θ domain from 6 to 65°. The reflection intensities were extracted from 769 frames recorded with standard exposure times of 30 s at a crystal-detector distance of 50 mm. The cell parameters were determined and refined with all of the integrated peaks using the Xcalibur CrysAlis software.[9] The main crystallographic details and the experimental parameters are given in Table 1.

The Orthorhombic $SmGa_{3.64}$ Phase. The set of 37 159 reflections (including symmetry-equivalent and redundant ones) recorded over the complete sphere diffraction was indexed in the orthorhombic F-centered cell of parameters $a = 8.493(1)$, $b = 14.912(2)$, and $c = 17.078(2)$ Å. The reflections were corrected for absorption effects ($\mu = 41.83$ mm^{-1}) using the SCALE3ABS numerical procedure included in the CrysAlis RED software. The data set used for final refinement in the *Fmmm* orthorhombic space group consisted of 1033 independent reflections ($R_{int} = 3.84\%$), of which 860 were observed according to the criterion $I > 2\ \sigma(I)$. The structure was solved by direct methods with the program SHELXS97;[10] three Sm and five Ga positions were assigned and isotropically refined with SHELXL97[11] to a reliability factor of ~10%. Free refinement of occupation factors indicated an incomplete filling of Sm1, Ga4, and Ga5 sites. Three high-intensity remaining peaks in the subsequent Fourier difference were found abnormally close to the latter positions; they were assigned to Ga6, Ga7, and Sm4 atoms with partial occupations. Within the standard deviation limits, site occupations freely converged in such a manner that Ga6 and Ga7 complemented Sm1 and that Sm4 complemented Ga4 and Ga5. This accounts for a statistical disorder (Figure 1) in which Sm1 and Sm4 at 8h sites are partially replaced by gallium triangles (Ga6−Ga7−Ga7 and Ga5−Ga4−Ga4, respectively). Thereafter, all of these site occupancies were refined using appropriate linear constraints. All atoms but Ga6, Ga7, and Sm4 with small occupations were refined with anisotropic atomic displacement parameters.

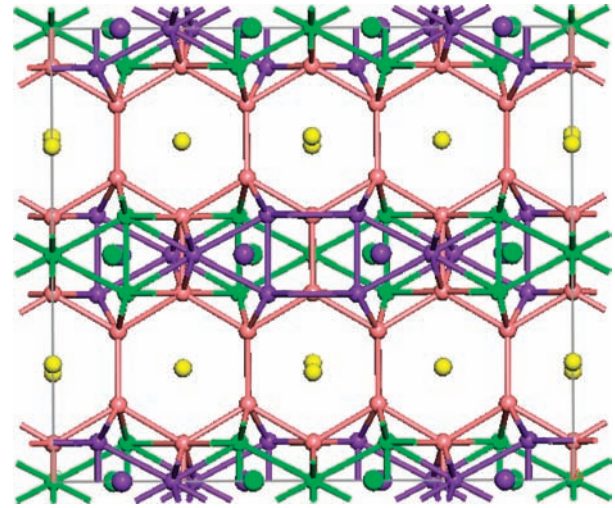

Figure 1. Crystal structure of $SmGa_{3.64}$ projected along the [100] direction. Atoms Sm1 (violet) and Sm4 (green) are partially replaced by gallium triangles Ga6−Ga7−Ga7 (violet) and Ga4−Ga4−Ga5 (green), respectively.

The final refinement on F^2 yielded a reliability factor R1 of 3.94% and a composition of $Sm_{0.98}Ga_{3.57}$ (or $SmGa_{3.64}$) in agreement with the energy dispersive X-ray (EDX) analysis. In any case, the occurrence of disorder could be attributed to a missed larger unit cell, a wrong space group, or even some twinning.

The Hexagonal $SmGa_{2.67}$ Phase. The 3425 (including symmetry-equivalent and redundant) reflections recorded under normal conditions within the complete diffraction sphere were indexed in a trigonal cell of parameters $a = 7.424(1)$ and $c = 4.2176(6)$ Å.

(9) *CrysAlis 'Red' 171*; Oxford Diffraction Ltd.: Abingdon, United Kingdom.
(10) Sheldrick, G. M. *SHELXS97*; University of Göttingen: Göttingen, Germany, 1997.
(11) Sheldrick, G. M. *SHELXL97*; University of Göttingen: Göttingen, Germany, 1997.

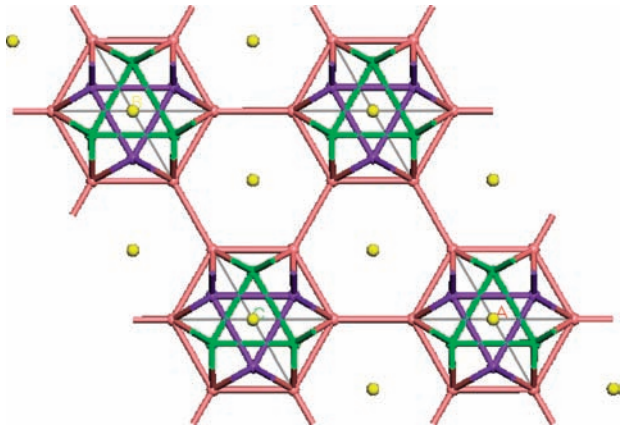

Figure 2. The basic trigonal cell of $SmGa_{2.79}$ ($a = 7.424$, $c = 4.218$ Å). Owing to $P312$ symmetry, the Sm1 atom at (0,0,1/2) is partially replaced by disordered (60° rotation) Ga triangles.

The structure was solved in space group $P312$ by direct methods; three Sm and two Ga positions were found and subsequently refined. Atom Sm1 at (0,0,1/2) lies inside a hexagon of Ga2 (site $x,-x,1/2$) giving too short distances (Sm1−Ga2 and Ga2−Ga2 of about 1.45 Å). The disorder represented in Figure 2 was taken into account by varying complementarily the occupations of Sm1 and Ga2. Finally, the structure was refined to a reliability factor R1 of 3.48% using a data set corrected for absorption effects ($\mu = 42.2$ mm^{-1}) consisting of 465 unique reflections, of which 318 were observed with $I > 2\sigma(I)$.

The refined composition $SmGa_{2.79}$ roughly agrees with the semiquantitative EDX analyses (Sm/Ga ratio close to 0.37) of several single crystals formerly characterized by X-ray diffraction (XRD).

The single crystal previously used for data collection was mounted again on the CCD diffractometer for a new data collection using longer exposure times (80 s per frame instead of 30). A total of 19 637 reflections (including symmetry-equivalent and redundant) were then indexed in a larger hexagonal cell, $a' = 12.861(2)$ and $c' = 8.4402(8)$ Å, related to the former trigonal cell by

$$\begin{pmatrix} a' \\ b' \\ c' \end{pmatrix} = \begin{pmatrix} 1 & -1 & 0 \\ 1 & 2 & 0 \\ 0 & 0 & 2 \end{pmatrix} \times \begin{pmatrix} a \\ b \\ c \end{pmatrix}$$

The intensities of reflections averaged correctly in the $P6/mmm$ Laue group ($R_{int} = 8.04\%$) as in $6/m$, $\bar{3}m$, and $\bar{3}$ lower symmetries. The unique extinction condition for reflections h h l with 1 odd and the $|E^2-1|$ distribution unambiguously indicate the noncentrosymmetric space group $P\bar{6}2c$. The structure was then solved in this space group from direct methods and refined to an R1 factor of 5.40% with a data set consisting of 1466 unique reflections, of which 985 were observed ($I > 2\sigma(I)$). Although most of the disorder problems were eliminated, some statistical atomic substitution still persisted, with two Sm atoms at (0,0,1/4) and (1/3,2/3,3/4) partially replaced by Ga triangles. The final refined composition, $SmGa_{2.67}$, is now in better agreement with the Sm/Ga ratio obtained from EDX analyses. The hexagonal crystal structure of $SmGa_{2.67}$ is represented in Figure 3.

To exclude any ambiguity concerning the existence of Ga_3 triangles in $SmGa_{2.67}$ that might have appeared as a consequence (*artifact*) of the imposed hexagonal symmetry, we solved and refined the structure successfully in the noncentrosymmetric triclinic space group P1, where triangular units were still found to substitute partially for Sm atoms.

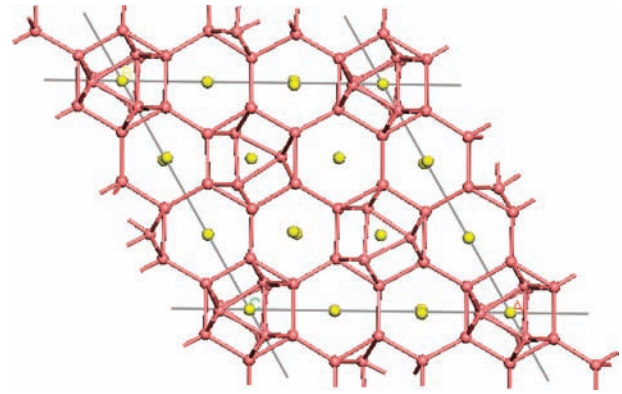

Figure 3. The hexagonal supercell of $SmGa_{2.67}$. The atomic disorder at the Ga triangles has been partially fixed and only subsists at sites (0,0,1/4) and (1/3,2/3,3/4), where there is some statistical replacement of Sm atoms by Ga triangles.

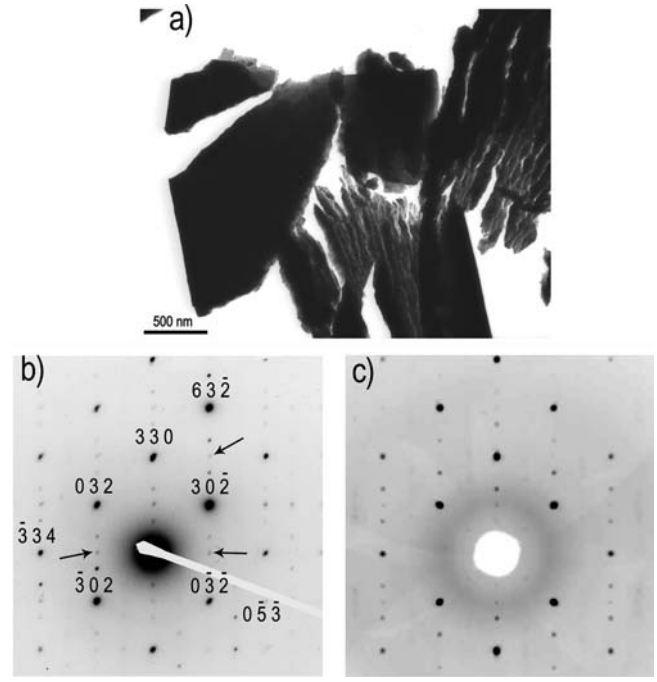

Figure 4. (a) TEM image from $SmGa_{2.67}$. (b) The [2 $\bar{2}$ 3] zone axis electron diffraction pattern: the diffraction spots are indexed in the hexagonal cell ($a = 12.861$, $c = 8.44$ Å). Weak extra diffraction spots indicated by arrows suggest further doubling of the cell along a and b. (c) Representation of the reciprocal lattice reconstructed from long exposure X-ray diffraction frames viewed along the same direction.

Because the flux synthesis method gave crystals of which surfaces are soiled by gallium, $SmGa_{2.67}$ was also prepared by direct synthesis from elements taken in the stoichiometric proportion. Large columnar hexagonal single crystals were obtained and identified as $SmGa_{2.67}$ by X-ray diffraction and EDX analyses. Transmission electron microscopy (TEM) experiments were carried out on a Jeol 200CX operating at 100 kV. Two sampling methods were used: mechanical grinding into small particles of about 100 nm dispersed in heptane and then collected on a carbon-coated copper grid or microtome slicing after incorporation of the crystal, carefully aligned along a preferential direction, into a resin. Electron diffraction patterns (Figure 4) are in agreement with the X-ray analysis; however, they display some weak extra diffraction spots, suggesting further doubling of the cell along a and b ($a = 25.72$ Å). These extra reflections were also detected on longer-exposure X-ray diffraction frames. Their number was too small and their

counting statistics too bad to make possible a full structural determination in this larger supercell.

Calculation Methods

Spin-polarized calculations were performed at the DFT level with VASP and DMOL3 codes using the gradient-corrected GGA approximation and the exchange and correlation functional PW91.[12] Accurate geometry optimizations were carried out with VASP,[13−15] which uses a plane-wave basis set, and the projector augmented wave technique, which aims to achieve simultaneously the computational efficiency of the pseudopotential method as well as the accuracy of the full potential linearized augmented plane wave method. In the standard mode, VASP treats the valence electrons in a scalar relativistic approximation.

DMOL3 is a DFT program that utilizes localized atomic orbitals to expand the electronic states.[16−18] The localized numerical orbitals used as basis sets (DND, double numerical plus a polarization *d*-function) are designed to give maximum accuracy for a given basis set size. There are some advantages associated with the use of such bases, particularly in the description of bonds and calculation of Mulliken charges.

Density functional semi-core pseudo-potentials have been used; they are a convenient way to introduce scalar relativistic effects into a formally nonrelativistic approach. For Ln lanthanide elements (Ln = La, Sm, Yb), $5s^25p^64f^N6s^2$ electrons were treated as valence electrons. The inner 3d levels of Ga were also considered as valence states. Kinetic cutoff energies were set at fine qualities. The Brillouin zone was sampled by Monkhorst−Pack[19] sets of *k* points with spacing between the grid points always less than 0.05 $Å^{-1}$.

Because most density functionals used nowadays (LDA, GGA) take the (near free) electron gas as input, they are expected to properly work only for slowly varying charge densities; they perform badly for lanthanides with rather compact 4f shells. Though these localized 4f electrons largely contribute to physical properties, they participate very little in bonding. Electronic effects resulting from "open shell" f orbitals with strongly correlated electrons yield bad SCF convergence and geometry optimizations for samarium compounds. To avoid convergence drawbacks, most of the calculations were carried out with isostructural phases containing lanthanum, an f electron-free element. Calculations were also performed for the ytterbium compound $YbGa_{2.64}$ with a 4f closed shell.

Structural Description

The structures of two new compounds have been determined whose stoichiometries, $SmGa_{3.64}$ and $SmGa_{2.67}$, are within the limits of the ε-$SmGa_x$ single-phase domain ($2 < x < 4$) given in the binary phase diagram.[2] Owing to disorder occurrence, the structure of $SmGa_{3.64}$ was solved in the orthorhombic *Fmmm* space group, while that of $SmGa_{2.67}$ was found to be hexagonal $P\bar{6}2c$. The atomic arrangements in these two structures are strongly reminiscent of the framework of $SmGa_2$ (*P6/mmm*, $a = 4.238$, $c = 4.187$ Å)[20−22] with a planar hexagonal layer of gallium in which the Ga hexagon is capped on both sides by a samarium atom (AlB_2 structural type). A slightly Sm-deficient variant[23] of $SmGa_2$ has been reported and its structure described in a C-centered orthorhombic cell ($a = 4.25$, $b = 7.37$, $c = 4.19$ Å).

The hexagonal $P\bar{6}2c$ structure of $SmGa_{2.67}$ ($a = 12.861(2)$, $c = 8.4402(8)$ Å) is built on a $3 \times 3 \times 2$ superstructure of $SmGa_2$ where, according to stoichiometry, Ga_3 units statistically substitute for some samarium atoms. In this structure, disorder occurs through atoms Sm4 and Sm5, which respectively occupy 2b and 2d sites with 27% and 64% filling, while the remaining atoms fully occupy their sites (Sm1 at 2c, Sm2 and Sm3 at 6 h). The slight waving of the gallium hexagonal layer results from Ga−Ga bonding between triangles and hexagonal layers. A different way to describe the whole gallium network is to consider a packing of interconnected Ga_{15} units (D_{3h} symmetry) built of two hemicuboctahedra fused by triangle sharing (see below).

The structure of $SmGa_{3.64}$ (*Fmmm*, $a = 8.493(1)$, $b = 14.912(2)$, $c = 17.078(2)$ Å) represented in Figure 1 is built of puckered hexagonal sheets of gallium stacked along the *a* axis. One half of the Sm atoms lying in the interlayer space are involved in statistical disorder: Sm1 and Sm4 occupy, respectively, 86.5 and 6.5% of their 8i sites, while Sm2 and Sm3 fully occupy 8c and 8h sites. At the 8i sites, Ga triangles partially substitute for Sm atoms. Like in $SmGa_{2.67}$, bonding of the Ga_3 triangular units to the Ga hexagonal network is responsible for the rather strong waving of layers. With a composition that is one-third of the way from $SmGa_{2.67}$ to $SmGa_6$, $SmGa_{3.64}$ represents a structural transition between two types of substitution: Ga triangles in $SmGa_{2.67}$ and Ga dumbbells in the Ga-richer $SmGa_6$ phase (Figure 5). While barycenters of Ga_3 units in $SmGa_{2.67}$ coincide with the Sm positions they substitute for, in $SmGa_{3.64}$, these Ga_3 triangles are isosceles and consistently shifted within the (100) plane from the Sm position.

In conclusion, the two phases derive from $SmGa_2$ by a progressive modification of the hexagonal Ga framework through the replacement of Sm atoms according to the substitution rate, as follows: $SmGa_2$ (0%), $SmGa_{2.67}$ (25%), $SmGa_{3.64}$ (45%), and $SmGa_6$ (66%).

Noteworthy is the different structural description given for phases ranging from ε-RGa_x (R = rare earth, $2 < x < 4$) to the tetragonal (*P4/nbm*) gallium-richer compound RGa_6.[21,24] With the increasing Ga content, the structure still retains the

(12) Perdew, J. P.; Chevary, J. A.; Vosko, S. H.; Jackson, K. A.; Pederson, M. R.; Singh, D. J.; Fiolhais, C. *Phys. Rev. B: Condens. Matter Mater. Phys.* **1992**, *46*, 6671.
(13) Kresse, G.; Forthmuller, J. *Phys. Rev. B: Condens. Matter Mater. Phys.* **1996**, *54*, 11169.
(14) MedeA-VASP (Materials Design Inc.) is a commercial pack that provides a graphical interface to set up, run, and analyze VASP calculations under the Windows environment.
(15) Kresse, G.; Forthmuller, J. *J. Comput. Mater. Sci.* **1996**, *6*, 15.
(16) Delley, B. *J. Chem. Phys.* **1990**, *92*, 508.
(17) Delley, B. J. *J. Phys. Chem.* **1996**, *100*, 6107. DMOL3 is distributed inside the commercial pack: *Materials Studio*, version 3.1.0; Accelrys Inc.: San Diego, CA, 2004.
(18) Delley, B. J. *Int. J. Quantum Chem.* **1998**, *69*, 423.
(19) Monkhorst, H. J.; Pack, J. D. *Phys. Rev. B: Condens. Matter Mater. Phys.* **1977**, *16*, 1748.
(20) Yatsenko, S. P.; Semenov, B. G.; Chuntonov, K. A. *Russ. Metall. (Engl. Transl.)* **1977**, *6*, 149–151.
(21) Kimmel, G.; Dayan, D.; Zevin, L.; Pelleg, J. *Metall. Trans. A* **1985**, *16*, 167–171.
(22) Haszko, S. E. *Trans. Metall. Soc. AIME* **1961**, *221*, 201–204.
(23) Grin, Y.; Fedorchuk, A. A. *Izv. Akad. Nauk SSSR, Met.* **1992**, *5*, 206–209.
(24) Pelleg, J.; Kimmel, G.; Dayan, D. *J. Less-Common Metals* **1981**, *81*, 33–44.

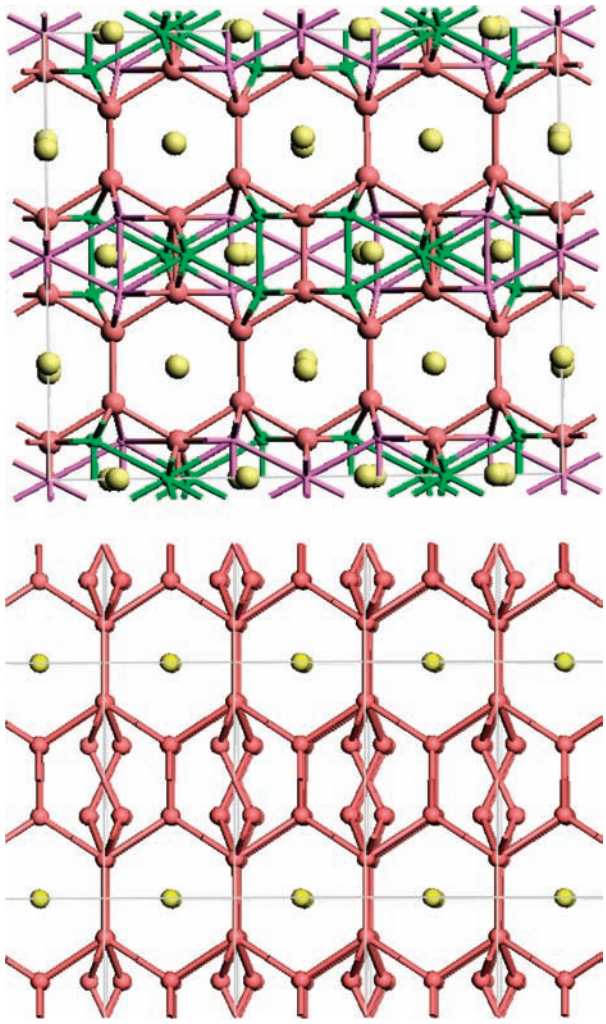

Figure 5. The orthorhombic $SmGa_{3.64}$ (up) and tetragonal $SmGa_6$ (down) structures. Sm atoms are represented in yellow.

Ga hexagonal layer present in RGa_2 (AlB_2 type), with R atoms continuously replaced, not by Ga triangles as was found in present work, but by Ga_2 dumbbells (*"pair-wise substitution of R atoms by Ga atoms"*). These structural arrangements lead, especially when R = Gd, Tb, Dy, Ho, and Er, to unlikely Ga−Ga distances of 2.29−2.15 Å (see Table 3 in ref 21).

Modelization and Electronic Structures

First, we shall focus on $SmGa_2$, for which the ordered structure is the basis of the gallium-richer compounds. The calculated band structure is represented in Figure 6 and partial densities of states in Figure 7.

The projected atomic density of states shows the 4f bands split by 0.15 Ha into two narrow bands on both sides of E_F. The main bonding contribution to the total DOS in the Fermi level domain is from the Ga p orbitals that provide both σ and π Ga−Ga bonding. The analysis of the molecular orbitals from a calculation at Γ indicates that the pseudo-degenerate and partially filled states (LUMO) just above the Fermi energy display marked π-bonding character (Figure 8). They would accept extra electrons without significant structural modification, underlining the adaptative behavior of the

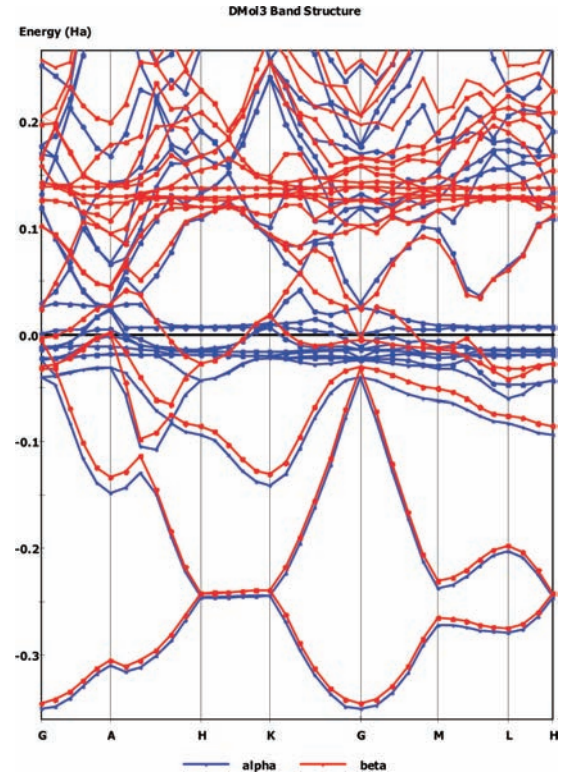

Figure 6. DMOL3 band structure for $SmGa_2$.

widespread AlB_2 structural type to a particular valence electron count.

Let us now examine how the basis structure of $SmGa_2$ is modified when some Sm atoms are randomly replaced by triangular gallium units to form $Sm_{1-x}Ga_{2+3x}$. The present hexagonal structure of $SmGa_{2.67}$ determined by XRD ($P\bar{6}2c$, a = 12.861, c = 8.4402 Å) corresponds to a 3 × 3 × 2 supercell of $SmGa_2$. To model the disorder with respect to the exact stoichiometry $SmGa_{2.67}$, we should consider a 6 × 6 × 6 supercell of $SmGa_2$ ($Sm_{216}Ga_{432}$) with 26 Sm atoms replaced by Ga_3 units, leading to the formula $Sm_{190}Ga_{510}$. The treatment of such a problem by DFT is obviously out of our computational capabilities. Since these structural modifications raise some interesting questions relative to the configuration and to the orientation of the Ga_{15} units (see further in the text for details), we used simpler models with a stoichiometry rounded to $SmGa_3$. They derive from a 3 × 3 × 2 supercell of $SmGa_2$ through the replacement of three Sm atoms with gallium triangles, and so they contain 15 Sm and 45 Ga atoms. Three ordered structural models with different packings of interconnected Ga_{15} units were analyzed: 3D-like alternate packing (AP), 2D-like layered packing (LP), and 3D-like columnar packing (CP) (Figure 9).

Note that, owing to much higher disorder, no such calculations could have been performed for the orthorhombic phase $SmGa_{3.64}$.

These models were geometry-optimized with VASP using La instead of Sm to avoid convergence problems. The substitution of La for Sm is also justified by the existence

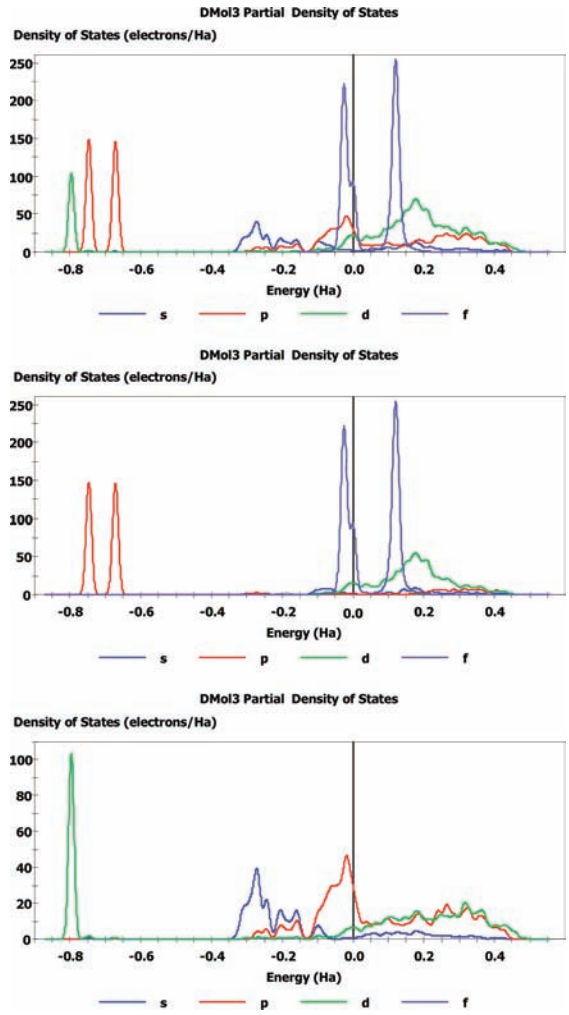

Figure 7. DMOL3 partial densities of states for all atoms (up), for samarium (middle), and for gallium (down) atoms in $SmGa_2$.

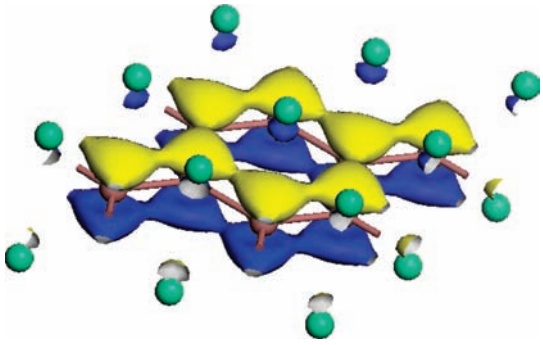

Figure 8. Representation of the pseudo-degenerate and partially filled molecular orbital (LUMO) of $SmGa_2$ displaying some π-bonding character.

of the phase $La_{0.89}Ga_{2.22}$ displaying a very close structure.[25] The latter was determined from powder data in the hexagonal space group (*P6/mmm*, $a = 4.36$, $c = 4.42$ Å) and found to be awfully disordered owing to the underestimation of cell parameters which are submultiples (1/3, 1/3, 1/2) of the present ones. In the $La_{0.89}Ga_{2.22}$ structure, the Ga_3 units are in the same orientation as in $SmGa_{2.67}$ but undergo 60° rotational disorder.

As indicated by the total energies obtained from VASP for the optimized geometries, the stability increases from CP to LP (by 0.12 eV/atom) and from LP to AP (by 0.04 eV/atom), a trend which is also found with DMOL3 calculations.

The phase $YbGa_{2.64}$ was described in space group *P6/mmm*, with $a = 13.025$ and $c = 8.36$ Å;[26] it was found consistently disordered with an overall atomic arrangement of the AP type very close to that in $SmGa_{2.67}$. The main difference stems from the Ga_{15} unit's new configuration, where the Ga_3 triangle rotates by 30° around the 3-fold axis, lowering the coordination inside the hexagonal prism (Figure 10). Owing to its *P6/mmm* symmetry, the structure of $YbGa_{2.64}$ contains one Ga_{15} unit at site D_{6h} with duplicated (by 60° rotation) triangles, while no such disorder is observed for the second unit at the D_{3h} site. Why do Ga_{15} units adopt configuration I in the La and Sm phases and configuration II in the Yb phase? Is this a consequence of relative atomic sizes or of different electron transfer effects?

In order to compare the relative stabilities of the two configurations (I and II), we have built periodic hexagonal models for the idealized $LaGa_3$ compound: in space group $P\bar{6}2m$ with configuration I as in $SmGa_{2.67}$ and in space group $P\bar{6}m2$ with configuration II as in $YbGa_{2.64}$. Geometries were optimized using VASP (*P1* symmetry, full cell and atomic relaxations). The optimized cell parameters $a = 13.127$ and $c = 8.711$ Å for configuration I and $a = 13.150$ and $c = 8.711$ Å for configuration II do not deviate more than 4% from the experimental ones. The calculated energies of formation are not significantly different, with a very small advantage for configuration I found in $SmGa_{2.67}$ (−228.09 kJ/mol against −227.96 kJ/mol). Atomic Mulliken populations were further calculated with DMOL3 using the geometries optimized by VASP. Mulliken charges for La atoms range from +1.6 to +1.9 (configuration I); they are practically identical for configuration II (+1.7 to +1.9). Charges on Ga atoms range from −0.24 to −0.27 on triangles and from −0.57 to −0.72 within the hexagons. In the nonsubstituted ordered $SmGa_2$ structure, Mulliken charges are +1.5 for Sm and −0.75 for Ga. Owing to the disordered structures of $SmGa_{2.67}$ and $YbGa_{2.64}$, their electronic properties are not as accessible as for $SmGa_2$. Let us now consider the computed Mulliken charges for the idealized $SmGa_3$ and $YbGa_3$ models of $SmGa_{2.67}$ and $YbGa_{2.64}$. The Sm charges are in the range +1.9 to +2.2 and those of Yb between +1.6 and +2.5; they differ significantly from the La charges only for the upper values. This discrepancy in charges results from the environments of the lanthanide elements by Ga_3 units. In $YbGa_3$, Yb atoms which are surrounded by three units (Yb−Ga: 3.05 Å) bear the highest charge, while those in contact with only one (Yb−Ga: 3.17 Å) or even no Ga_3 unit have the lowest charges.

As indicated by the rather short bonds, some covalent bonding occurs within the gallium frameworks of $SmGa_{2.67}$ and $YbGa_{2.64}$; the whole three-dimensional structure could be described as formed with individual Ga_{15} units (two hexagons sandwiching a triangle). These units would be 12-

(25) Lu, X. S.; Xie, S. S.; Liang, J. K. *Wuli Xuebao* **1982**, *31*, 1635–1641.

(26) Cirafici, S.; Fornasini, M. L. *J. Less-Common Metals* **1990**, *163*, 331–338.

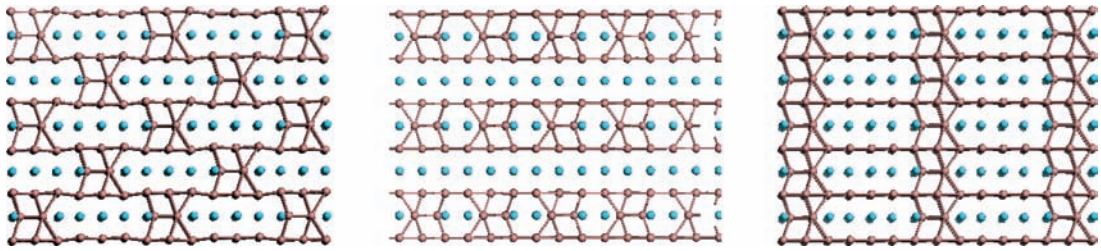

Figure 9. 3D-like alternate packing (AP), 2D-like layered packing (LP), and 3D-like columnar packing (CP) involving Ga_{15} units. These units are interconnected through direct bonding (AP and LP) and through direct bonding and hexagon sharing (CP).

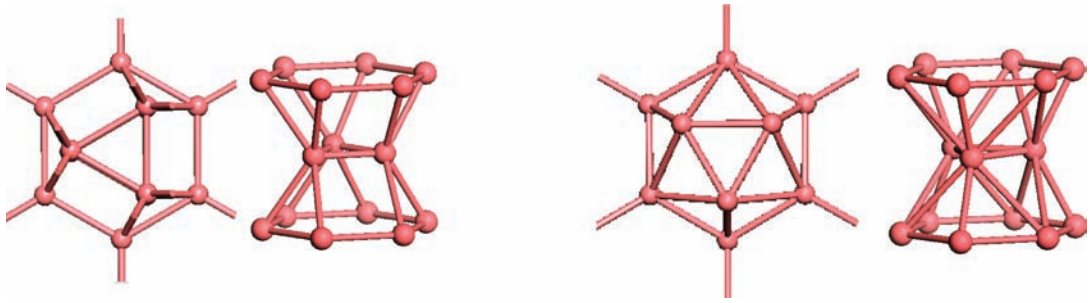

Figure 10. The two possible configurations for Ga_{15} units (projection and front view) for configuration I (left) and configuration II (right).

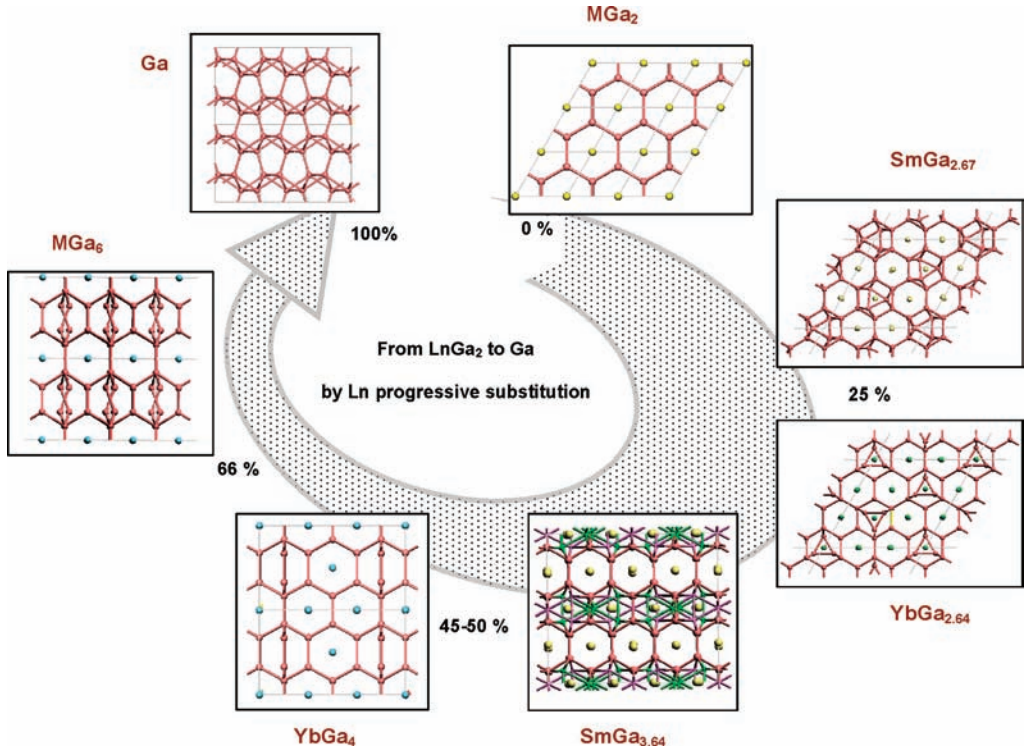

Figure 11. Ln-rich domain of Ln−Ga diagrams: structural evolution starting from composition $LnGa_2$ to $LnGa_6$ due to the progressive replacement of lanthanide atoms by gallium atoms.

fold exocoordinated through rather short classical 2c−2e bonds of about 2.5 Å.

Concluding Remarks

The understanding of the gallium-rich domain of the phase diagram between lanthanide elements and gallium remained a challenging problem until the update in the Yb−Ga system.[28] The La and Sm phase diagrams have not been revised since their first publication, mainly because of the lack of good crystal structure determinations. In these diagrams, the acute question relates to the existence and boundaries of the so-called ε phase (*P6/mmm*). The ε phase is supposed to exist between $LaGa_2$ and $LaGa_{4.56}$ and between $SmGa_2$ and the uncertified $SmGa_4$ composition (dotted line). For system Sm−Ga, the present work unveils two new crystal structures ($SmGa_{2.67}$ and $SmGa_{3.64}$) solved and refined in respective $P\bar{6}2c$ and *Fmmm* space groups. Surprisingly,

(27) Ren, J.; Liang, W.; Whangbo, M. H. *CAESAR 2.0 package for Windows*; North Carolina State University: Raleigh, NC, 2002.

(28) Yb-Ga phase diagram assessed from: *J. Phase Equilib.* **1992**, *13* (1).

these compositions lie inside the boundaries of a domain formerly assumed to be single-phased. The present structural work brings evidence that the ε-phase domain in the Sm−Ga system is also narrow, like in the Yb−Ga system with $YbGa_{3-x}$ ($0 \leq x \leq 0.35$). In Figure 11 is represented the evolution of the structures starting from composition $LnGa_2$ (2D graphite-like Ga framework) and moving to $LnGa_6$ (3D cyclohexane-like distorted Ga framework) by the progressive replacement of Ln (Ln = Sm, Yb) with Ga atoms. For both types of lanthanide elements, the evolution looks almost parallel up to the formation of the pure gallium (orthorhombic) phase, except at substitution rates of 45−50%, where $SmGa_{3.64}$ (*Fmmm*) and $YbGa_4$ (*I*4/*mmm*) have different structures. Recently, another compound, $YbGa_5$, noncongruently melting, has been added between $YbGa_4$ and $YbGa_6$.[29] At a substitution rate of 25%, the $SmGa_{2.67}$ and $YbGa_{2.64}$ structures are very close, with the only difference regarding the orientation of the Ga_3 units that substitute for lanthanide elements.

Supporting Information Available: A crystallographic file in CIF format. This material is available free of charge via the Internet at http://pubs.acs.org.

IC801379C

(29) Giedigkeit, R.; Niewa, R.; Schnelle, W.; Grin, Y.; Kniep, R. *Z. Anorg. Allg. Chem.* **2002**, *628*, 1692–1696.